

# Comparison of several Riemann solvers applied to the polytropic Euler's equations

Guoxiang(Grayson) Tong

Adviser: Prof. Jed Brown

## I. Introduction

Euler's equation is a typical model for studying nonlinear hyperbolic conservation laws, and it is a simplified version of the famous Navier-Stokes equation. To numerically solve the hyperbolic PDEs, the finite volume method presents its robustness of dealing with the physical phenomena created by shocks, rarefactions or other contact discontinuities.

In 1978, Gary A. Sod<sup>8</sup> investigated several finite volume methods applied to the 1-D Euler's equation. In this paper, the numerical performances of a few famous difference schemes like the methods named after Godunov, Lax-Wendroff, MacCormack, Rusanov, Glimm, and a traditional upwind scheme were compared, and in the end, the Glimm's method was favored in the sense of its high resolution near the discontinuous regions.

The physics behind this paper is a 1-D shock tube problem with the polytropic gas, and the corresponding system of equations can be written as:<sup>8</sup>

$$\rho_t + (\rho u)_x = 0 \quad (1)$$

$$m_t + (m^2/\rho + p)_x = 0 \quad (2)$$

$$E_t + ((m/\rho)(E + p))_x = 0 \quad (3)$$

Where  $\rho$  is the density of the gas;  $m = \rho u$  stands for the momentum and the  $E = \rho e + \frac{1}{2}\rho u^2$  is the unit energy per volume with  $e$  being the internal energy. By the equation of state for the polytropic gas, the energy  $E$  can also be written as:

$$E = \frac{p}{\gamma - 1} + \frac{1}{2}\rho u^2 \quad (4)$$

and the pressure  $p$  can be computed as:

$$p = \frac{\rho c^2}{\gamma} = (\gamma - 1)(E - \frac{\rho u^2}{2}) \quad (5)$$

where  $\gamma \approx 1.4$  as the heat capacity ratio, and the  $c$  is the speed of sound. Considering the state variables  $\rho$ ,  $m$  and  $E$  can be expressed as a "vector" with three components, thus the conservation law of this problem is shown as:

$$\mathbf{U}_t + \mathbf{F}(\mathbf{U})_x = 0 \quad (6)$$

where the state vector  $\mathbf{U} = [\rho, m, E]$  and the flux vector  $\mathbf{F}(\mathbf{U}) = [m, m^2/\rho + p, (m/\rho)(E + p)]$ . However, In computation, rather than analyzing the behaviour of the conserved state quantities  $\rho, m, E$ , the variables  $\rho, u$  and  $p$  are often studied in the Riemann problem.<sup>9</sup> Then, in the consideration of the non-linearity of this problem, the Jacobian matrix needs to be computed as:<sup>3</sup>

$$J(\mathbf{U}) = \begin{bmatrix} 0 & 1 & 0 \\ \frac{1}{2}(\gamma - 3)u^2 & (3 - \gamma)u & \gamma - 1 \\ \frac{1}{2}(\gamma - 1)u^3 - u\frac{E+p}{\rho} & \frac{E+p}{\rho} - (\gamma - 1)u^2 & \gamma u \end{bmatrix} \quad (7)$$

Thus the conservation law(6) can also be written as  $\mathbf{U}_t + J(\mathbf{U}) \cdot \mathbf{U}_x = 0$ , and the eigenvalues of  $J(\mathbf{U})$ :  $\lambda_1 = u - c$ ,  $\lambda_2 = u$  and  $\lambda_3 = u + c$  represent for the three waves with their associated speeds (where the  $c$  is not a constant but rather computed as  $c = \sqrt{\frac{\gamma p}{\rho}}$ ). Besides, by the nonlinear study,<sup>3</sup> the waves with the speed  $u + c$  and  $u - c$  show “genuine non-linearity”, while the rest wave with speed  $u$  leads to the linear degeneracy of the system, and as a result, a contact discontinuity will occur and cause a density jump across this region. By the analysis above, four possible wave structures may appear as the left and the right nonlinear waves being either shock or rarefaction with the middle wave being the contact discontinuity.

For the sake of testing the ability of handling the discontinuity, a specific initial condition is established.<sup>8</sup> At time  $t = 0$ , the density  $\rho$  and the pressure  $p$  on the two sides of the interface  $x = 0.5$  have a jump as  $\rho_1 = 1$ ,  $\rho_2 = 0.125$  and  $p_1 = 1$ ,  $p_2 = 0.1$ , while the gas itself being static as  $u_1 = u_2 = 0$ . Then, as time evolves, this state is broken and the variables change spatially. Furthermore, note that only the status in the neighborhood of the discontinuity will be investigated thus the periodic boundary condition is established with a relatively larger domain.

In this project, the focus lies on the Riemann problem, in addition to the exact Riemann solver, several famous approximate solvers, the HLL(C) solver, the Ruasnov’s method, and the Roe’s(Roe-Pike) method will be implemented to the same 1-D Euler’s equation, aiming to realize parts of the result in this highly-cited paper.

As for the discretization, the 1-D domain is set as  $x \in [-1, 2]$  with the uniform grid size  $\Delta x = 0.01$ ; the time iteration will apply the 5th-order Runge-Kutta-Fehlberg<sup>1</sup> method with an adaptive error control, in which the tolerance is set as  $err = 10^{-5}$  and the  $\Delta t = 0.005$  for the initial time step size. Moreover, in order to reduce the effect of oscillations, slope reconstruction will be implemented to each solver based on the Minmod flux limiter by Roe(1986).<sup>6</sup>

In all the solvers, the time for comparison is  $t \approx 0.25s$ . At this time, there are exact solutions of the density, velocity, pressure and internal energy from Toro’s book,<sup>9</sup> where the data is said to be extracted from Sod’s work.<sup>8</sup> However, in Sod’s original paper,<sup>8</sup> the exact output time for the comparison plots is not declared, thus, in this project, the data from Toro’s book<sup>9</sup> will be used as the exact solution.

## II. The HLL(C) and Ruasnov solvers

The approximate solvers applied in this part are the HLL(Harten-Lax-Van Leer)<sup>2</sup> solver, the Rusanov solver,<sup>7</sup> and the HLLC(Harten-Lax-Van Leer-Contact)<sup>9</sup> solver. Theoretically, the former two assume that only

two shocks will occur in the problem, while the latter one also takes the existence of a contact wave into consideration. Except for the supersonic cases, where the upwind flux will be used, the HLL method computes the sonic flux as:

$$\mathbf{F}_{HLL}(\mathbf{U}_*) = \frac{s_R \mathbf{F}_L - s_L \mathbf{F}_R + s_L s_R (\mathbf{U}_R - \mathbf{U}_L)}{s_R - s_L} \quad (8)$$

In Rusanov's scheme, it will be computed as:

$$\mathbf{F}_R(\mathbf{U}_*) = \frac{1}{2}(\mathbf{F}_L + \mathbf{F}_R) - \frac{s}{2}(\mathbf{U}_R - \mathbf{U}_L) \quad (9)$$

And finally in HLLC solver,<sup>9</sup> where the possible contact discontinuity will be restored, thus the variables inside the “star” regions should be computed. Specifically, based on the assumption that the contact wave also being a shock with the shock speed  $S_*$ , and the Rankine-Hugoniot condition, two additional possible fluxes are calculated as:

$$\mathbf{F}_{HLLC}(\mathbf{U}_*)_L = \frac{S_*(S_L \mathbf{U}_L - \mathbf{F}_L) + S_L P_{LR} \mathbf{D}_*}{S_L - S_*} \quad (10)$$

$$\mathbf{F}_{HLLC}(\mathbf{U}_*)_R = \frac{S_*(S_R \mathbf{U}_R - \mathbf{F}_R) + S_R P_{LR} \mathbf{D}_*}{S_R - S_*} \quad (11)$$

where the  $S_L$ ,  $S_R$ ,  $S_*$  are the left, right and central shock speeds, respectively.  $P_{LR}$  is an averaged pressure in the “star” regions and the  $\mathbf{D}_*$  is an auxiliary vector defined as:  $\mathbf{D}_*[i] = [0, 1, S_*[i]]$ .

The results of these three approximate Riemann solvers with respect to the exact solutions in the paper are as Figure1:

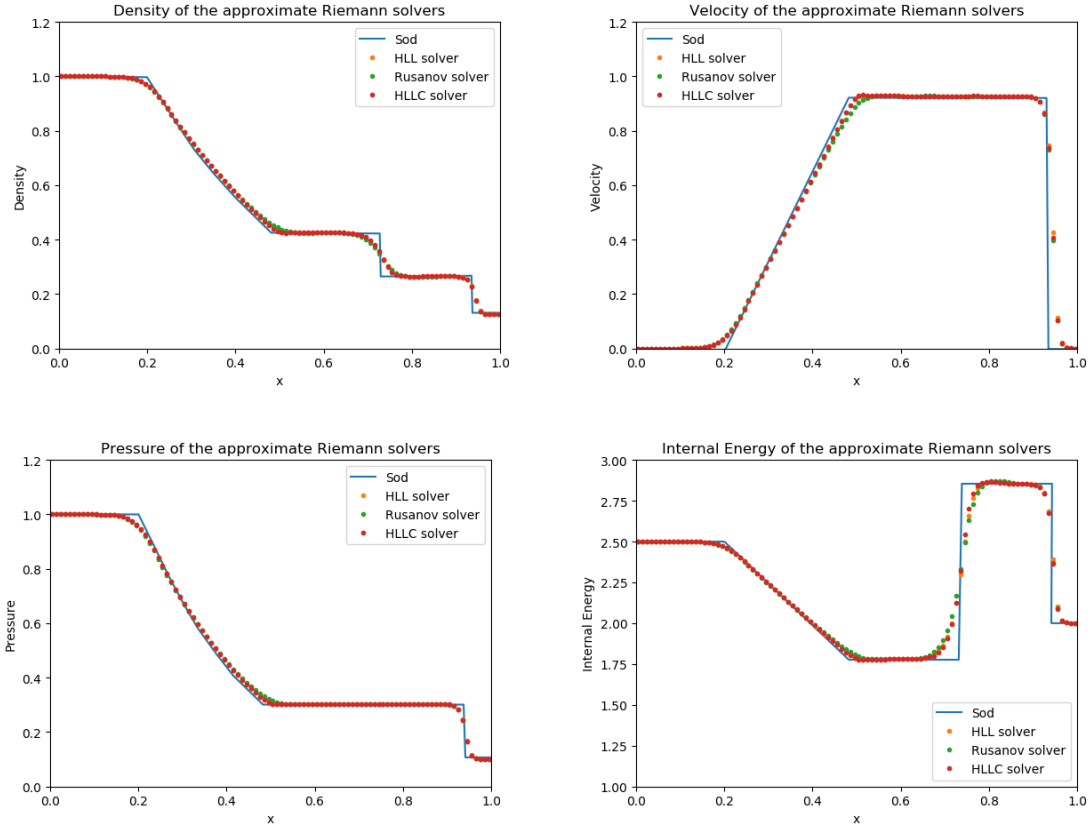


Figure 1. Results of the approximate Riemann solvers

Comparing to the exact solutions from the paper, we can see relatively good approximations in all the three methods. Besides, the HLLC scheme is slightly better than the other two cases which could be observed in the velocity subfigure. However, the corners of the exact results are not achieved in all three solvers, especially when it comes to the computation of internal energy.

From the construction of these methods, we know that all possible wave structures are assumed as shocks or contact waves, and thus the lack of rarefaction considerations may result in a relatively large numerical diffusivity.

### III. The Roe's(Roe-Pike) method

The Roe's method<sup>5</sup> is also a famous Riemann solver where the intercell fluxes are approximated by the averaged quantities  $[\cdot]$ , and the Jacobian matrix  $J(U)$  will be decomposed into its eigenspace with those averaged values. Finally, the output flux of Roe's method can be computed as<sup>9</sup>(Chapter.11):

$$\mathbf{F}_{Roe} = \frac{\mathbf{F}_L + \mathbf{F}_R}{2} - \frac{\sum_{i=1,2,...,m} \tilde{\alpha}_i \tilde{\lambda}_i \tilde{\mathbf{K}}_i}{2} \quad (12)$$

In terms of the problem in this paper, the eigenvalues  $\tilde{\lambda}_i$  and their associated eigenvectors  $\tilde{\mathbf{K}}_i$  as:

$$\begin{aligned} \tilde{\lambda}_1 &= \tilde{u} - \tilde{c}, \tilde{\mathbf{K}}_1 = [1, \tilde{u} - \tilde{c}, \frac{\tilde{E} + \tilde{P}}{\tilde{\rho}}] \\ \tilde{\lambda}_2 &= \tilde{u}, \tilde{\mathbf{K}}_2 = [1, \tilde{u}, \frac{\tilde{u}^2}{2}] \\ \tilde{\lambda}_3 &= \tilde{u} + \tilde{c}, \tilde{\mathbf{K}}_3 = [1, \tilde{u} + \tilde{c}, \frac{\tilde{E} + \tilde{P}}{\tilde{\rho}} + \tilde{u}\tilde{c}] \end{aligned}$$

Then the the averaged "wave strengths"  $\tilde{\alpha}_i$  can be obtained by the solving the below formula:

$$\mathbf{U}_R - \mathbf{U}_L = \sum_{i=1,2,3} \tilde{\alpha}_i \tilde{\mathbf{K}}_i \quad (13)$$

Additionally, if eigenvalues and eigenvectors are approximated directly by the averaged primal variables  $\rho, u, p$  rather than by decomposing the averaged Jacobian matrix, then the Roe's scheme turns to the approach by Roe and Pike.<sup>4</sup>

The Figure2 presents the results of the Roe's and the Roe-Pike's method. Similar as the HLL(C) family, the profiles of all quantities have been smoothed so that the "corner" structures generated by the discontinuities are not achieved. Moreover, for the physics of this problem, it can be observed that the results of these two methods are highly similar.

### IV. The exact Riemann solver

In this part, an exact Riemann solver will be utilized, where the computations of all wave structures that may occur are embedded in the solver. As the aforementioned analysis, the special eigenstructure makes four regions existing in this exact Riemann problem, i.e. the left and right regions outside the nonlinear waves and two "star" areas divided by the contact discontinuity. Clearly, the left and right states can be obtained just by sampling the indices, while the crucial "star" regions must be computed by the nonlinear iterative solver.

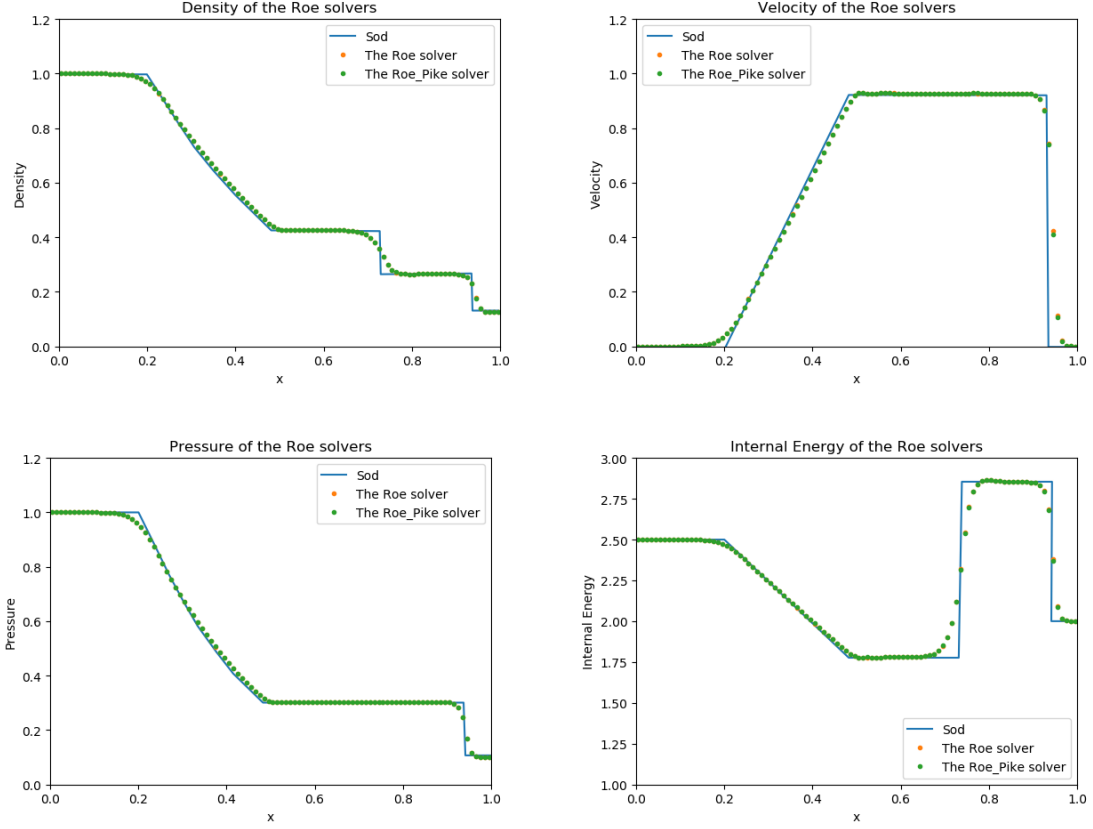


**Figure 2. Results of the Roe's method**

In this part, our theoretical work is based on the conclusions in Toro's book<sup>9</sup>(Chapter.4), where the non-conserved variables  $u_*$  and  $p_*$  are calculated in the “star” regions with the value of  $p_*$  being an indicator of determining the type of a nonlinear wave. Considering the  $p_*$  and  $u_*$  will not have a jump across the contact discontinuity, thus the algebraic equations based on  $p_*$  and  $u_*$  is derived as:

$$f_L(p_*, \rho_L, u_L, p_L) + f_R(p_*, \rho_R, u_R, p_R) + u_R - u_L = 0 \quad (14)$$

$$u_* = \frac{u_L + u_R}{2} + \frac{[f_R(p_*, \rho_R, u_R, p_R) - f_L(p_*, \rho_L, u_L, p_L)]}{2} \quad (15)$$

Where  $f_L$  and  $f_R$  have different expressions in the sense of the nonlinear waves being a shock or a rarefaction, and the explicit definitions of  $f_L$  and  $f_R$  can be found in Toro's book(equation 4.5-4.9).<sup>9</sup>

After obtaining the  $p_*$ , the last state variable  $\rho_*$  can be derived directly from its left or right state along with the  $p_*$  inside the “star” regions, but it also depends on whether a shock or rarefaction the nonlinear wave is. Then, in the course of computing the fluxes, the local sound speed  $c_*$ , and possible shock speeds  $S_L$  or  $S_R$ , and the possible rarefaction speeds(including the head and tail speeds  $R_H$ ,  $R_L$ ) are all calculated inside the “star” region for the purpose of determining the exact flux vector in each cell.

In the course of sampling the flux to each cell, the Riemann Invariant relationship<sup>9</sup> defined as:

$$u_L + \frac{2a_L}{\gamma - 1} = u_0 + \frac{2a_0}{\gamma - 1} \quad (16)$$

is used to determine the state variables  $\rho_0$ ,  $u_0$  and  $p_0$  inside of a sonic rarefaction region. Then the upwind or downwind flux will be sampled when a supersonic shock or rarefaction occurs, and finally inside the “star” regions, whether  $\rho_{*L}$  or  $\rho_{*R}$  will be used is decided by the its nearby shock or rarefaction speed.

Results of the exact solver are shown in Figure3. Comparing to the approximate Riemann solvers in the Figure1 and Figure2 above, the corner structures are much better preserved in the exact solvers. However, unfortunately, the time discretization in this exact solver requires much finer step size, which is initially set to be  $\Delta t = 0.0005$  and otherwise, the exact method can be quite unstable. In addition, it can be said that this solver is not a “complete” exact Riemann solver, for the density sampling of the star region is just assumed to take the average of  $\rho_{*L}$  and  $\rho_{*R}$ . Similarly, if the individual value is taken, the method will be unstable as well. Thus, it is likely that the weird oscillations in the density and internal energy subfigures could attribute to the assumptions above.

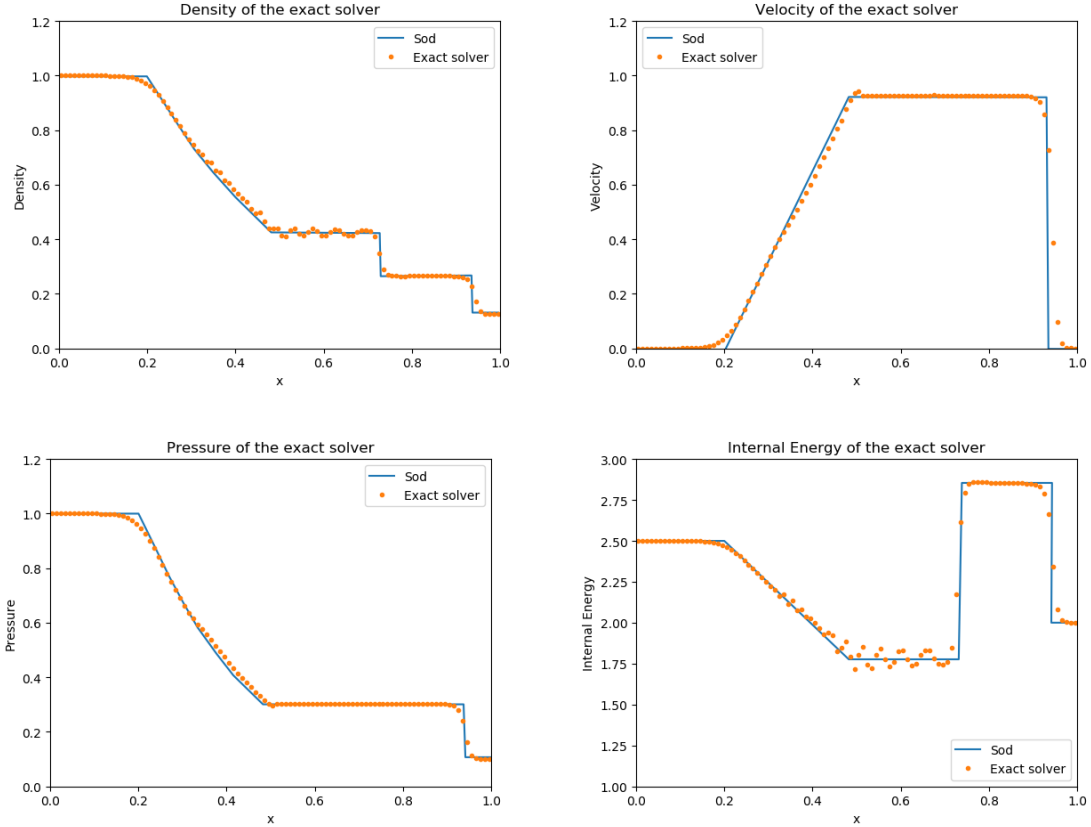


Figure 3. Results of the exact Riemann solvers

## V. Comparison on a finer grid

In this section, the performance of the three typical methods, the HLLC method, the Roe-Pike method, and the exact Riemann solver are investigated in a finer spatial and temporal discretization as  $\Delta x = 0.005$

and  $\Delta t = 0.0005$ . The purpose of this experiment aims to find the best approximation in the sense of an "optimal" setting. The results are plotted in Figure4, and the time required of each computation is recorded as: HLLC(43.8564s), Roe-Pike(35.3275s), Exact(74.74s).

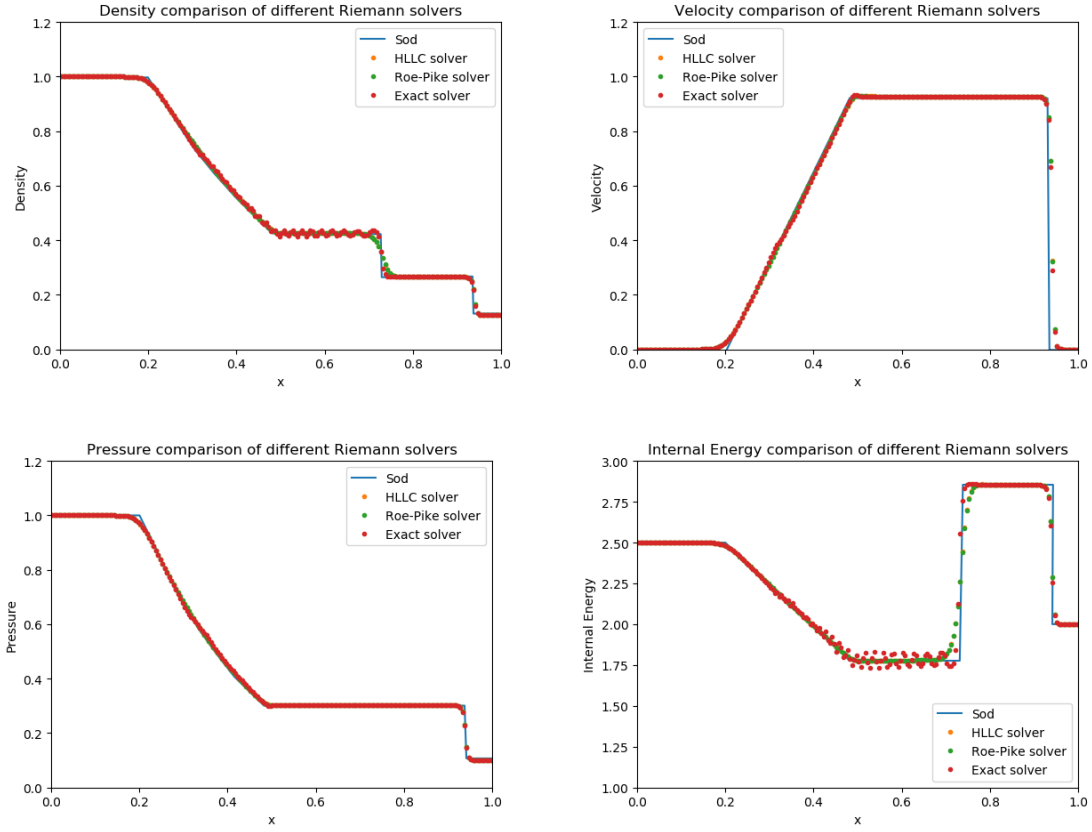


Figure 4. Comparison of different Riemann solvers

In the approximations of velocity and pressure, all three methods work well with only a little over-smoothness near the corners. While for the density and internal energy, it appears that the exact solver does a better job than the other two, for the "stage" structures are relatively preserved. However, the unsteady oscillations still deteriorate the exact solver especially in the case of the internal energy. Also, we can see much time is also required for the exact solver, therefore, in the case of this problem, the approximate Riemann solvers may be eligible to replace the exact one.

## VI. Future work

- 1: The solution sampling of the star regions in the exact solver needs to be revised for the sake of avoiding the unwanted ripples.
- 2: According to Sod,<sup>8</sup> the high-resolution Glimm's method will have a better approximation near the discontinuities, which can be implemented and compared with the exact Riemann solver.
- 3: The multi-dimensional Euler's equation can also be written as a conservation law and solved by the notion of a Riemann problem. At that time, more waves will appear so the cases for choosing numerical fluxes could

be much more difficult. Thus, a possible future work will start with a 2-D problem with also the polytropic gas.

## VII. Acknowledgments

The python code and the theoretical work in this project are partly based on the notes and lectures by Prof. Jed Brown in the course CSCI 5636-001. Special gratitude is given to professor Brown for his detailed guidance in this project and the excellent teaching in this semester.

## References

- <sup>1</sup>Erwin Fehlberg. Klassische runge-kutta-formeln vierter und niedrigerer ordnung mit schrittweiten-kontrolle und ihre anwendung auf wärmeleitungsprobleme,. *omputing (Arch. Elektron. Rechnen)*, vol. 6, pp. 61–71, 1970.
- <sup>2</sup>P.D. Harten, A.and Lax and B. van Leer. On upstream difference and godunov-type schemes for hyperbolic conservation laws,. *SIAM Review*, 25, 35-61., 1983.
- <sup>3</sup>Randall J. LeVeque. Finite volume methods for hyperbolic problems,. *Cambridge University Press*, 2002.
- <sup>4</sup>P. L. Roe and J. Pike. Efficient construction and utilisation of approximate riemann solutions,. *Computing Methods in Applied Science and Engineering. North-Holland*, 1984.
- <sup>5</sup>Philip L Roe. Approximate riemann solvers, parameter vectors, and difference schemes,. *J. Comput. Phys.*, 43:357–372,, 1981.
- <sup>6</sup>Philip L Roe. Characteristic-based schemes for the euler equations,. *Annual review of fluid mechanics* 18 (1), 337-365, 1986.
- <sup>7</sup>V.V . RUSANOV. Calculation of interaction of non steady shock waves with obstacles,. *J. Comp. Math. Phys.*, vol. 1, pp. 267-279,, 1961.
- <sup>8</sup>Gary A. Sod. A survey of several finite difference methods for systems of nonlinear hyperbolic conservation laws. *Journal of Computational Physics, Volume 27, Issue 1, Pages 1-31*, 1978.
- <sup>9</sup>Eleuterio F Toro. Riemann solvers and numerical methods for fluid dynamics-a practical introduction. *Springer*, 2009.